Desalination and Water Treatment
www.deswater.com
doi: 10.5004/dwt.2021.27435

230 (2021) 219–226
August

Oxidation of sulfur ions in oilfield wastewater by montmorillonite loaded Mn catalyzed hydrogen peroxide oxidation

Zhongying Xu[a], Jianlong Dong[a], Yifan Liu[a,b], Jie Zhang[a], Chengtun Qu[a,b], Ying Tang[a,b,*]

[a]*Shaanxi Province Key Laboratory of Environmental Pollution Control and Reservoir Protection Technology of Oilfields, Xi'an Shiyou University, Xi'an, China, emails: tangying78@xsyu.edu.cn (Y. Tang), 834690660@qq.com (Z. Xu), 1042149738@qq.com (J. Dong), zhangjie@xsyu.edu.cn (J. Zhang), xianquct@xsyu.edu.cn (C. Qu)*
[b]*State Key Laboratory of Petroleum Pollution Control, CNPC Research Institute of Safety and Environmental Technology, Beijing, China, email: 1804196485@qq.com*

Received 30 January 2021; Accepted 15 May 2021

ABSTRACT

In this paper, the sulfur ions in oilfield wastewater were treated by oxidation to harmless elemental sulfur or high valence sulfur-containing organics using hydrogen peroxide catalyzed by montmorillonite-loaded manganese oxides (B@Mn) as a catalyst. The effects of pH, hydrogen peroxide dosage, reaction time, and temperature on sulfide removal were studied separately. The results show that the best reaction conditions were achieved when the simulated wastewater concentration was 25.6 mg/L (pH = 8) and the molar ratio of hydrogen peroxide to sodium sulfide was 5.1:1 (T = 30°C). Under the optimal conditions, the sulfide ion concentration of the B@Mn-4 catalyst was reduced to 0.0225 mg/L. Further, the morphology and pore structures of catalyst were studied in detail using various characterization methods including scanning electron microscopy, UV-vis spectrophotometry, thermogravimetric, and N_2 adsorption–desorption analysis.

Keywords: Hydrogen peroxide; Sulfur ions; Oxidation desulphurization

1. Introduction

Along with the increase in oil and gas field production, there has been an increase in wastewater from oil fields with high valence sulfur-containing organics [1–2]. Sulfur ions in oilfields mainly come from sulfur-containing crude oil and sulfate produced by biomass metabolism [3]. Sulfide has strict emission standards (Class I standard sulfide 1 mg/L) because of its strong corrosive, toxic, and odor characteristics [4–6]. A portion of the oilfield wastewater was treated and recycled for use as oilfield injection water, while another portion was discharged into the environment after meeting treatment standards [7]. The strategies currently used to remove sulfides including membrane separation, physical adsorption [8], nitrate method [9], dissolved oxygen oxidation [10], iron salt precipitation [11], desulfurization agent desulfurization, etc. In addition to a single application, some of them are used in combination to obtain a better removal effect [12]. Of course, there are also some removal methods, such as biological removal, which are very effective in removing sulfides [13]. Not only can it operate at atmospheric pressure and low temperatures without additional chemical costs, but some methods require high levels of experimental equipment and reactions, which indirectly drive up the economic costs [14]. As a result, conventional wastewater treatment methods can only remove most of the oily substances, and the removal of sulfides was not complete.

* Corresponding author.

From an economic point of view, the removal of sulfides from wastewater is quite expensive, so it is crucial to develop an optimal non-toxic catalyst for the treatment of sulfur-containing wastewater [15–16]. With the advent of advanced oxidation technologies (AOPs), oxidative desulfurization (ODS) has evolved towards the use of stronger oxidizers to remove sulfides from oilfield wastewater in the form of sulfates [17]. Hydrogen peroxide is widely used in medical, military, industrial, and other fields, and is called a green oxidizer because of its environmental protection, simple post-reaction treatment, and water by-product [18]. So wastewater treated with it as an environmentally friendly strong oxidizer was more easily biodegradable [19].

In this study, a composite B@Mn catalyst was prepared to oxidize the sulfur ions in the simulated sulfur-containing wastewater by hydrogen peroxide oxidation to harmless simple sulfur or high valent oxygenate to reduce the pollution hazard of sulfide.

2. Experimental

2.1. Chemicals and materials

Sodium sulfide was purchased from Bodi Chemical Co., (Tianjin, China). *N*,*N*-dimethyl-p-phenylenediamine hydrochloride was obtained from Aoran Fine Chemical Research Institute (Tianjin, China). Zinc acetate and sodium acetate were purchased from Dengfeng Chemical Reagent Factory (Tianjin, China). All reagents were of analytical grade. Deionized water was used for the preparation of the solutions throughout the experiment.

2.2. Sulfur ion content determination

Owing to the high sulfide concentration and pH in the wastewater, it was generally diluted by diluting the water sample during the experiment, although it was adjusted by adding acid if the pH was still high after dilution [20]. However, if not done properly, it can produce H_2S, which can be a serious threat to operator safety and is not available in production practice. The standard curve between divalent sulfur ions and absorbance was established by taking the concentration of divalent sulfur ions as the horizontal coordinate and the absorbance measured at a wavelength of 665 nm using a UV-vis spectrophotometer as the vertical coordinate. For an initial sodium sulfide and *N*,*N*-dimethyl-p-phenylenediamine hydrochloride concentration of 1 g/L and 0.001 mol/L, respectively. In the 100 mL volumetric bottle, 0.1 mL waste solution containing sulfur and 20 mL of zinc acetate-sodium acetate solution, 60 mL of distilled water were added to it. An addition of 10 mL of *N*,*N*-dimethyl-p-phenylenediamine solution was slowly added along the bottle wall, just after the addition of ammonium ferric sulfate solution 1 mL. Then, the solution was placed in the dark for 10 min and diluted with distilled water to the mark. Next, the absorbance was measured using a UV-vis spectrophotometer at 665 nm, and the sulfur ion concentration in the diluted wastewater was determined against a standard curve, and the sulfur ion removal rate was calculated according to the following equation:

$$C_0 = \frac{\left(A + 0.0041\right)}{0.0198} \tag{1}$$

$$\eta = \frac{C_0 - C_a}{C_0} \tag{2}$$

where C_0 (mg/L) is the initial sulfur ion concentration, C_a (mg/L) is the sulfur ion concentration measured under different conditions, A is the absorbance, and η (%) is the sulfur ion removal rate.

2.3. Catalysts preparation

In this experiment, the aqueous solution prepared by mixing K_2MnO_4 and montmorillonite in a certain proportion was treated by the impregnation method [21]. The mixed solution was dried in an air oven at 105°C after stirring for 30 min. Under the condition of fully removing the moisture, the muffle furnace was set at 550°C, 650°C, 750°C, and calcined for 4 h, then cooled and pulverized for storage. All the catalysts were named B@Mn-X, where X is the catalyst prepared under different conditions. The details were shown in Table 1. The load process is shown in Fig. 1.

2.4. Characterization of materials

Absorbance was measured using UV-vis spectrophotometer UV-2600 (Japan). The scanning electron microscopy (SEM, JSM-6390A, JEOL, Japan) was used to elucidate the morphology of the prepared materials at an accelerating voltage of 20.0 kV. The TG curves of the samples were recorded using a thermogravimetric analyzer TGA/DSC1 (METTLER TOLEDO, Inc., Switzerland) at an N_2 gas flow rate of 10 mL/min and a temperature rise rate of 10°C/min. The number and distribution of alkaline sites on the catalyst surface as well as the alkaline intensity were determined using a Micromeritics Chemisorb 2750 analysis.

3. Results and discussion

3.1. Effect of pH on sulfide removal efficiency

Removal of sulfur ions from oilfield wastewater by oxidation with hydrogen peroxide, which oxidizes them to harmless monomeric sulfur or highly valent oxygenated acid salts, thereby reducing the hazard level of sulfides. In the process of decreasing pH, a white colloidal sulfur

Table 1
Naming of catalysts

Temperature (°C)	Mass ratio	Named
550	10:1	B@Mn-1
	20:1	B@Mn-2
650	10:1	B@Mn-3
	20:1	B@Mn-4
750	10:1	B@Mn-5
	20:1	B@Mn-6

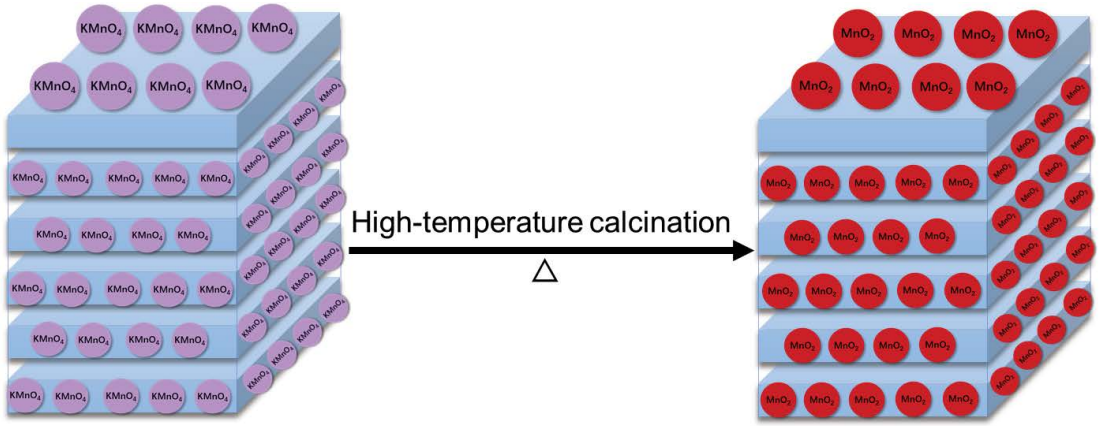

Fig. 1. Schematic diagram of montmorillonite reloading catalyst.

precipitate is generated, which makes the reaction solution turbid. The state of sulfur presence changes when pH regulation changes in the following equations:

$$S^{2-} + H_2O = HS^- + OH^- \quad (A)$$

$$SH^- + H^+ = H_2S \quad (B)$$

$$S_4^{2-} + H^+ = HS_4^- \quad (C)$$

$$SO_3^{2-} + H^+ = HSO_3^- \quad (D)$$

In this study, sulfur-containing wastewater was prepared by simulation, and the concentration of sulfide in the wastewater was 25.6 mg/L in terms of sulfur ions during the initial investigation, and the pH was adjusted by 0.1 mol/L hydrochloric acid solution and 0.1 mol/L sodium hydroxide solution during the experimental process. Under the conditions of a controlled initial temperature of 30°C and reaction time of 30 min, the effect of the pH of the solution on the sulfide removal rate was investigated by adjusting the pH of the solution. It was found that the high removal rate of sulfide ions and the effect of the simulated initial pH of the water were mainly related to the characteristics of hydrogen peroxide, as shown in the following two-electrode reaction:

$$H_2O_2 \rightleftharpoons H^+ + HO_2^- \quad (E)$$

$$HO_2^- + H_2O + 2e \rightleftharpoons 3OH^- \quad E^\theta = 0.87 \text{ V} \quad (F)$$

In acidic mediums:

$$H_2O_2 + 2H^+ + 2e \rightleftharpoons 2H_2O \quad E^\theta = 1.77 \text{ V} \quad (G)$$

The electrode potentials indicate that S^{2-} oxidation can be performed in both acidic and alkaline media and that Hydrogen peroxide is more oxidizable in acid, simulating that the sulfur ions in the water are more likely to escape in the form of hydrogen sulfide, making it more difficult for them in safety and handling, so treatment of sulfur ions under overly acidic conditions is not considered [22]. In conditions of alkalinity, the standard electrode potentials for sulfur in various states of existence were as follows: $E^0_A(S^{2-}/S)$ = –0.48 V, $E^0_A(S/S_2O_3^{2-})$ = –0.74 V, E^0_A ($S_2O_3^{2-}$/SO_3^{2-}) = –0.58 V, $E^0_A(SO_3^{2-}/SO_4^{2-})$ = –0.93V. The sulfur ion is the most reducible. Sulfur in each of the above valence states has certain reducibility, among which the divalent sulfur ion has the strongest redox property. It can undergo oxidation–reduction reactions with various oxidants to convert it into other non-toxic forms of sulfur.

Fig. 2 shows that 43% sulfide removal was achieved at pH = 6, this is mainly due to the presence of sulfides in the form of HS^- under acidic conditions. Therefore, only the pH of the solution can maintain the stable presence of sulfides under alkaline conditions. At pH = 13 in Fig. 2, the sulfide will exist in solution as an ion rather than in air, which is a relatively safe range. However, under strongly alkaline conditions, the hydrogen peroxide will decompose, the effective oxygen component will be reduced, the oxidation capacity will be weakened, which is not conducive to the reaction, resulting in a decrease in the sulfide removal rate. In summary, a pH of 8 was chosen.

3.2. Effect of molar ratio of H_2O_2 to Na_2S on sulfide removal effect

The following equation shows the reaction equation for the removal of sulfides by hydrogen peroxide oxidation at different ratios:

$$S^{2-} + H_2O_2 \rightarrow S + 2OH^- \quad (H)$$

$$S^{2-} + 4H_2O_2 \rightarrow SO_4^{2-} + 4H_2O \quad (I)$$

$$S^{2-} + 3H_2O_2 \rightarrow SO_3^{2-} + 3H_2O \quad (J)$$

$$2S^{2-} + 4H_2O_2 \rightarrow S_2O_3^{2-} + 3H_2O + 2OH^- \quad (K)$$

$$S + 2OH^- + 3H_2O_2 = SO_4^{2-} + 4H_2O \quad (L)$$

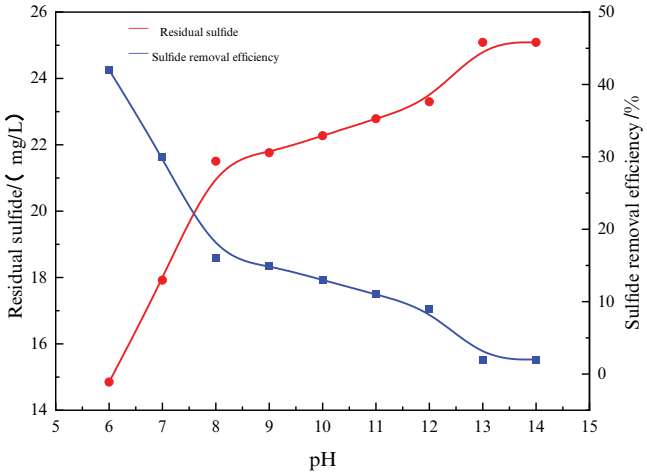

Fig. 2. Effect of pH value on removal efficiency of sulfur ion.

The standard electrode potentials obtained for each couple under acidic conditions are as follows:

$$E_A^0\left(S/HS^-\right) = -0.065\ V \quad (3)$$

$$E_A^0\left(S_2O_3^{2-}/HS^-\right) = 0.20\ V \quad (4)$$

$$E_A^0\left(H_2O_2/H_2O\right) = 1.776\ V \quad (5)$$

$$E_A^0\left(SO_4^{2-}/HS^-\right) = 0.251\ V \quad (6)$$

REDOX reaction can only occur when the electric potential of oxidation couples is greater than that of reduction couples, as the difference between the two increases, the more completely the reaction proceeds [23]. With the increasing molar ratio of hydrogen peroxide and sodium sulfide, the highly oxidizing reactive oxygen produced by hydrogen peroxide oxidizes the sulfide into a variety of intermediates combined with the adjacent sulfur to form S–S bonds, and with the increasing oxidation, the trend of forming S–S bonds weakens, and the trend of sulfur replacing lattice oxygen becomes larger, thus forming the end product sulfate.

It was clear from the reaction equation that at an initial hydrogen peroxide to sodium sulfide ratio of 4:1 (mol/mol), the reaction was slow and the sulfide removal was low. The reaction rate was fastest when the molar ratio of the reaction reaches 5.1:1 (mol/mol) and sulfide removal was maximized, but the sulfur ions will be present as sulfur monomers, thiosulfates, sulfites, and sulfates. At low molarity, the generation of monomeric sulfur was favored. Sulfate and thiosulfate were produced when the molarity was relatively high.

3.3. Effect of reaction time on sulfide removal

The effect of reaction time on the removal rate of sulfide under the conditions of control initial temperature of 30°C, hydrogen peroxide and sodium sulfide ratio of 5.1:1 (mol/mol), pH 8, and initial sodium sulfide of 25.8 mg/L. Fig. 3 shows that when the reaction time was between 10 and 40 min, the removal rate of sulfide increases with the increase of reaction time, and the growth rate was very fast. When the reaction time was 40 min, the removal rate reaches the maximum of 94.68%, and the mass concentration of sulfide in wastewater drops to 1.36 mg/L, which has reached the standard of gas field reinjection water.

It is noteworthy that the removal rate does not vary much between 10 and 40 min of reaction time. On the one hand, the reaction was rapid and reached equilibrium in a short time within 10 min. On the other hand, the concentration of hydrogen peroxide in the initial phase was very high, which is due to the high concentration of hydrogen peroxide at the initial stage of the reaction makes the reaction occur rapidly and can fully react, and the oxidation rate of sodium sulfide was large; the oxidation process occurs at close to room temperature, the system does not obtain energy from the outside world, the total number of activating molecules was fixed. The frequency was decreasing and the oxidation of hydrogen peroxide was almost complete.

3.4. Effect of temperature on the effectiveness of sulfide removal

Normally, the temperature of oilfield-produced water is not less than 30°C. In this study, temperature (30°C–70°C) was investigated as a factor affecting desulfurization. At reaction conditions of H_2O_2:Na_2S = 5.1:1 (mol/mol), pH = 8, for 40 min, with an initial Na_2S concentration of 25.6 mg/L, the law of the effect of temperature on sulfide removal rate was investigated. As can be seen from Fig. 4, the temperature at 30°C~50°C, the basic efficiency of sulfide removal did not change. It proves that the catalyst achieves a favorable removal effect at 30°C. When the temperature reached 70°C, the highest sulfide removal rate reached 99.47%, the mass concentration of sulfide in the sewage decreased to 0.135 mg/L. In actual oilfield sewage treatment temperature would not arrive at 70°C, the sulfur ion removal at a temperature of 30°C achieved about 96%, and the sulfide removal was already obvious.

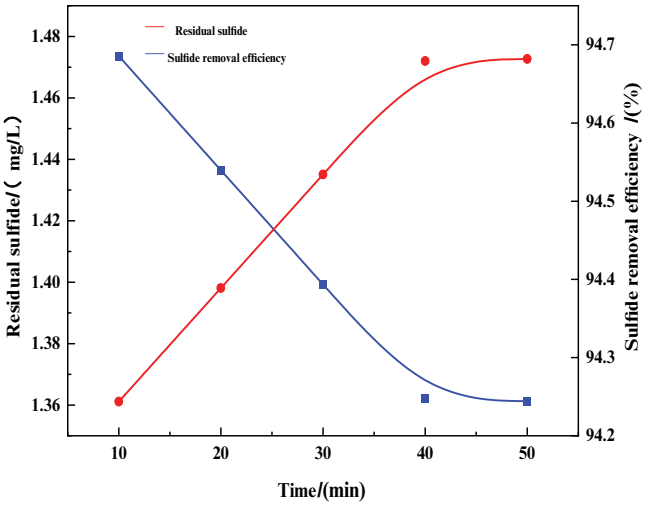

Fig. 3. Effect of reaction time on removal efficiency of sulfide.

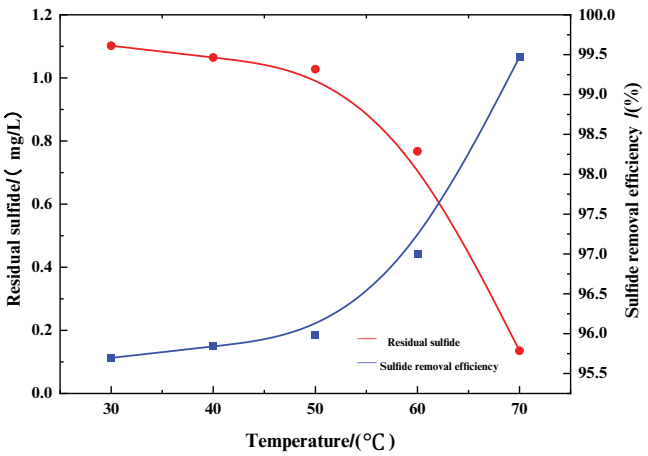

Fig. 4. Effect of temperature on removal of sulfur ions.

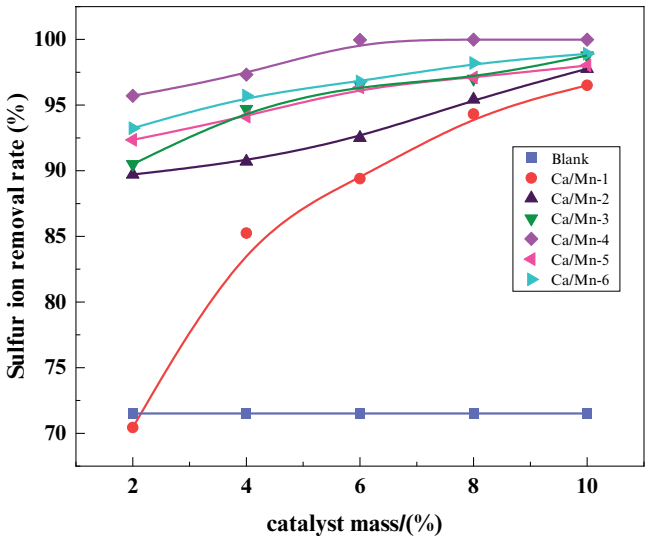

Fig. 5. Effect of catalyst and dosage on removal efficiency of sulfur ion.

3.5. Effect of catalyst-catalyzed hydrogen peroxide on the removal of sulfides

The effect of different catalysts on the sulfur ion removal rate was investigated based on previous experiments. At pH 8, H_2O_2:Na_2S = 5.1:1 (mol/mol), the reaction time of 40 min, and the reaction temperature of 30°C, the following conditions were used. From Fig. 5, it can be seen that all six catalysts have some influence on the removal rate of sulfur ions, and the sulfur ion removal rate of catalyst B@Mn-4 can reach 99.98% when the dosage reaches 6%. With the further increase of the catalyst concentration, the sulfur ion removal rate did not change significantly. In the blank sample, the sulfur ion removal rate was only 71.51% when calcium was added instead of the catalyst under the above conditions.

3.6. Effect of sulfide ion concentration on efficiency

Under the conditions of controlling the pH of simulated water as 8, H_2O_2:Na_2S = 5.1:1 (mol/mol), the reaction time as 40 min, the temperature as 30°C, and the catalyst selection with calcium Mn-4 at a mass fraction of 6% on the initial sulfur ion concentration size on the sulfur ion removal rate. It can be seen from Fig. 6, that the removal rate of sulfur ions decreases with the increase of the initial concentration of sulfur ions under the conditions of certain control reaction factors, but the decrease is small. When the initial concentrations of sulfur ions were set to 100; 400; 800; 1,200; 1,600; and 2,000 mg/L, the removal rates of sulfur ions could be obtained as 99.96%, 99.85%, 98.85%, 97.63%, 96.68%, and 96.25%, respectively. There was an effect of the initial concentration of the simulated water on the removal rate of sulfur ions. When the maximum concentration of sulfur ions was 2,000 mg/L, the removal rate could reach 96.25%.

3.7. Thermogravimetric analysis

From Fig. 7, it was known that montmorillonite and calcium Mn-4 under different temperature roasting, there was some loss in mass of montmorillonite, the mass of montmorillonite changed about 5% when the temperature

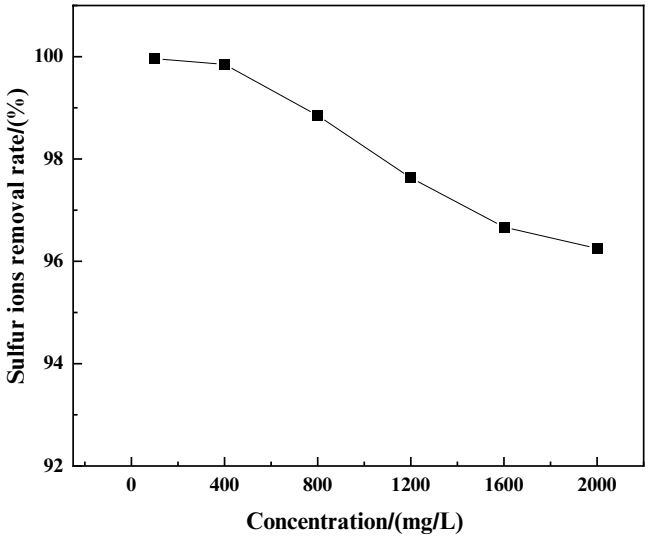

Fig. 6. Effect of sulfur ion concentration on removal rate.

was increased to 400°C, while the mass loss of catalyst after roasting was more than 20%. Some of the montmorillonite clay and airborne water molecules attached to the catalyst may be caused by the roasting temperature, and most importantly, $KMnO_4$ may not be completely decomposed to reach a stable state under the temperature change.

3.8. Catalyst chemisorption measurement

Fig. 8 shows that the amount of CO_2 desorption in the CO_2-TPD curve reflects, to some extent, the number of active sites on the surface of the catalyst calcium Mn-4, while the highest desorption temperature reflects the relative strength of the acid-base of the catalyst. The results of chemisorption characterization of the catalysts obtained at different roasting temperatures were different. The adsorption curves of

B@Mn-4 catalysts at 550°C, 650°C, and 750°C were mainly investigated in the above study. At 550°C, owing to the low firing temperature, only part of the $KMnO_4$ was decomposed by high-temperature oxidation, and the amount of MnO_2 produced was quite limited. From Fig. 7, we can see that the peak heights of the catalysts obtained after roasting at 650°C and 750°C were almost identical, and the peak areas were also roughly the same. and the comparison with the catalysts obtained after firing at 550°C was obvious. It also indicated that the number of basic sites on the catalyst surface was comparable for the catalysts roasted at 650°C and 750°C, and that different roasting temperatures have an effect on the basic sites on the catalyst surface, but they remain unchanged after reaching a certain value of temperature.

3.9. Particle size analysis

The average and median particle sizes of montmorillonite and B@Mn-4 after roasting at different temperatures are shown in Table 2. The average particle size of the hydrated calcium clay at room temperature was 12.32 μm, and the median particle size was 11.827 μm. However, the average and median particle sizes of the loaded catalysts increase somewhat, mainly due to the conversion of $KMnO_4$ to MnO_2 after high-temperature roasting and the adsorption of MnO_2 itself. Further indicating a significant loading effect was the average particle size of 15.234 μm and the median particle size of 13.211 μm for B@Mn-4 when roasted at 650°C. The average particle size of B@Mn-4 at 650°C was 15.234 μm and the median particle size was 13.211 μm.

3.10. SEM analysis

Fig. 9 shows SEM pictures of B@Mn-4 catalysts with different loadings. The morphology of the montmorillonite was mainly a lumpy structure of different sizes and scattered, when the loading was 10% of the catalyst began to condense into a whole, but the surface of the catalyst was still rough. When the load increases up to 20%, the catalyst starts to show a large amount of lumpy structure, MnO_2 itself has a certain adsorption and coagulation effect, this structure also indirectly verifies the effect of MnO_2 loading on montmorillonite.

3.11. XRD analysis

Fig. 10 presents the XRD spectra of the B@Mn-4 catalysts and bentonite. The XRD patterns from the bentonite samples indicate that the main composition of the bentonite was montmorillonite, with square quartz (SiO_2) as a secondary component. The catalyst composition consists mainly of MnO_2 (2θ = 12.75° and 29.09°) (JCPDS 72-1982) and montmorillonite (2θ = 20.90°, 26.73°, and 50.15°) (JCPDS 70-3755) crystalline phases. Meanwhile, the XRD pattern of montmorillonite shows sharp and intense reflections. The peak at 2θ = 12.75° can be indexed to δ-MnO_2 (JCPDS 72-1982). It was demonstrated that the MnO_2 generated after roasting

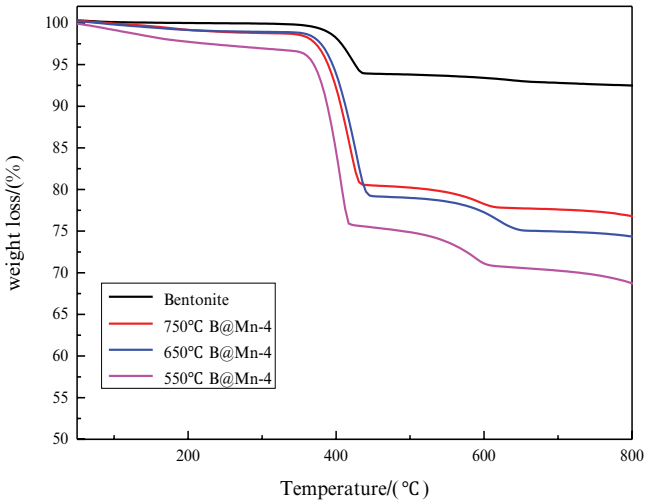

Fig. 7. TG curves of montmorillonite and calcium Mn-4.

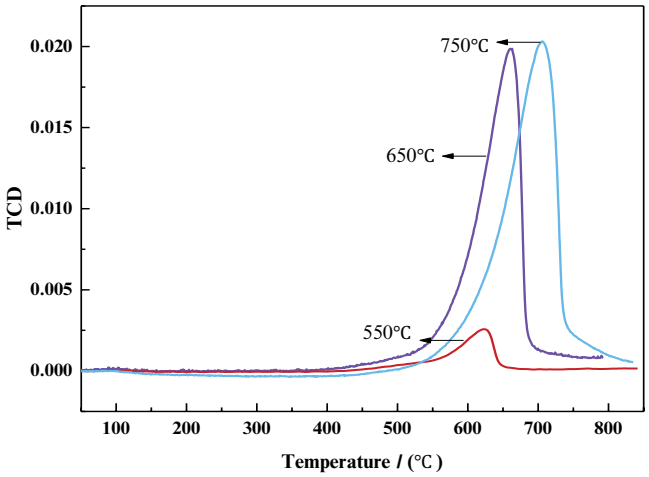

Fig. 8. CO_2-TPD curves of catalysts at different roasting temperatures.

Table 2
Mean diameter and median diameter of calcium soil B@Mn-4 at different temperatures

Temperature (°C)	Sample	Mean diameter (μm)	Median diameter (μm)
Room temperature	Montmorillonite	12.32	11.827
550	B@Mn-4	10.32	8.643
650	B@Mn-4	15.234	13.211
750	B@Mn-4	14.455	13.011

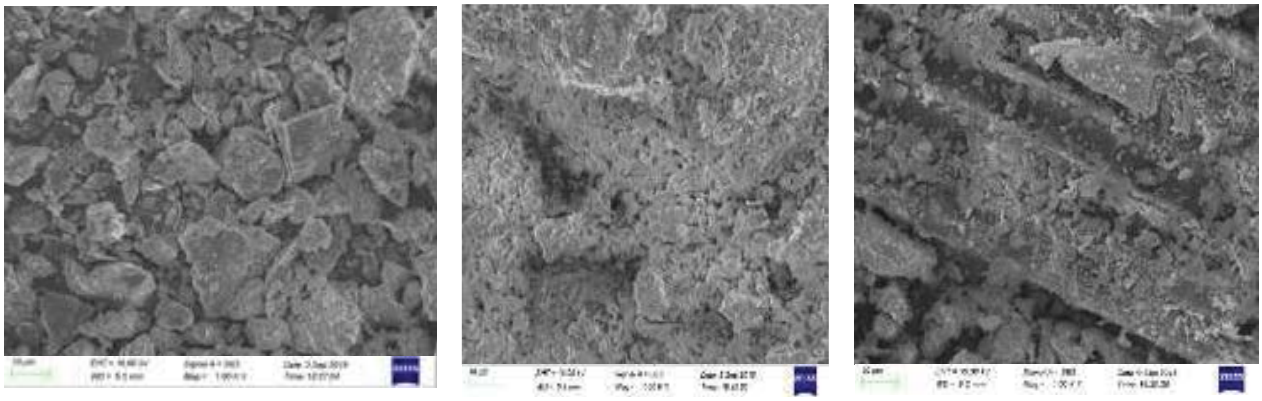

Fig. 9. SEM of B@Mn-4 catalyst with different loading: (a) hydrated montmorillonite, (b) 10% B@Mn-4, and (c) 20% B@Mn-4.

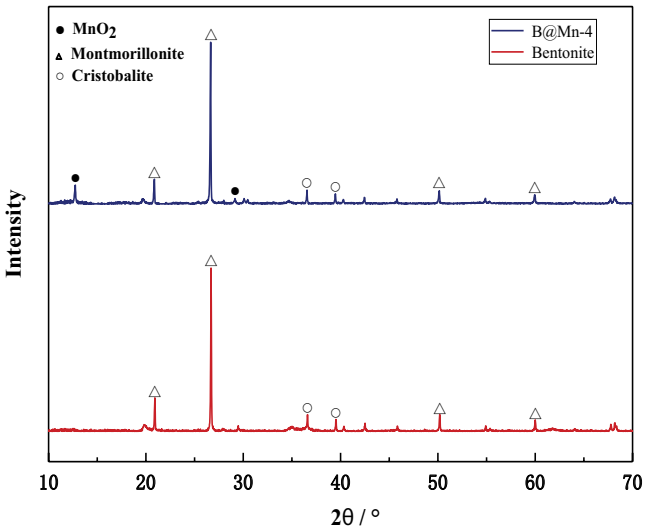

Fig. 10. XRD patterns of B@Mn-4 catalyst and bentonite.

of $KMnO_4$ was loaded on the montmorillonite, which corresponded to the SEM results.

4. Conclusions

In this study, B@Mn composite catalysts were successfully prepared to catalyze hydrogen peroxide oxidation for the treatment of sulfur ions in simulated sulfur-containing wastewater. The selection variables were optimized by examining the initial pH of the reaction, molar ratio, reaction time, temperature, and the amount of catalyst used. The reaction conditions with the best sulfur ion removal from the wastewater were identified. The experiments showed that the best results were obtained when the initial pH value of simulated water was 8, the reaction time was 30 min, the temperature was 30°C, H_2O_2:Na_2S = 5.1:1, and the catalyst was B@Mn-4. The removal rate of sulfur ions under these conditions was up to 99.97%, and the sulfur ion concentration was reduced to 0.0225 mg/L, which met the discharge standard of oilfield wastewater. Several characterization means were preferred to give the best catalytic effect of the catalyst B@Mn-4. Manganese dioxide loaded onto montmorillonite at a ratio of ten percent and roasted at 650°C for 4 h gave the best catalytic effect.

Competing interests

The authors declare that they have no competing interests.

Acknowledgments

The work was supported financially by the Youth Innovation Team of Shaanxi University, Shaanxi Provincial Key Research and Development Program (2019ZDLGY06-03), and the Postgraduate Innovation Fund Project of Xi'an Shiyou University (YCS20211023). We thank the work of the Modern Analysis and Testing Center of Xi'an Shiyou University.

References

[1] D.A. Agrawal, D. An, A. Cavallaro, G. Voordouw, Souring in low-temperature surface facilities of two high-temperature Argentinian oil fields, Appl. Microbiol. Biotechnol., 98 (2014) 8017–8029.
[2] H. Li, S. Niu, C. Lu, M. Liu, M. Huo, Transesterification catalyzed by industrial waste—lime mud doped with potassium fluoride and the kinetic calculation, Energy Convers. Manage., 86 (2014) 1110–1117.
[3] G. Zhu, S. Zhang, Q. Liu, J. Zhang, J. Yang, T. Wu, Y. Huang, S. Meng, Distribution and treatment of harmful gas from heavy oil production in the Liaohe Oilfield, Northeast China, Pet. Sci., 7 (2010) 422–427.
[4] Y. Gao, W. Zhu, C. Wang, X. Zhao, M. Shu, J. Zhang, H. Bai, Enhancement of oxygen reduction on a newly fabricated cathode and its application in the electro-Fenton process, Electrochim. Acta, 330 (2020) 135–206.
[5] Y.A. Khodor, T.M. Albayati, Employing sodium hydroxide in desulfurization of the actual heavy crude oil: theoretical optimization and experimental evaluation, Process Saf. Environ. Prot., 136 (2020) 334–342.
[6] W.H. Wu, Electrochemical corrosion prevention in oilfield wastewater for effective dissolved oxygen removal using a novel upflow bioelectrochemical system, Asian J. Chem., 6 (2019) 1–9.
[7] O. Tambwe, A. Kotsiopoulos, S. Harrison, Desulphurising high sulphur coal discards using an accelerated heap leach approach, Hydrometallurgy, 197 (2020) 465–472.

[8] Y. Liu, Y.H. Wang, J. Zhao, Y. Liu, C. Liu, Ultra-deep desulfurization by reactive adsorption desulfurization on copper-based catalysts, J. Energy Chem., 29 (2019) 16–24.
[9] R.A. Rodríguez, C.C. Jul, D. Gómez-Limón, Evolution of the organic sulfur and other components during nitric acid leaching of Mequinenza coal, Fuel, 76 (1997) 1445–1450.
[10] H.K. Namgung, J.H. Song, The effect of oxygen supply on the dual growth kinetics of *Acidithiobacillus thiooxidans* under acidic conditions for biogas desulfurization, Int. J. Environ. Res. Public Health, 12 (2015) 1368–1386.
[11] J. Yan, W. Yuan, J. Liu, W. Ye, J. Lin, J. Xie, X Huang, S. Gao, J. Xie, S. Liu, W. Chen, H. Zhang, An integrated process of chemical precipitation and sulfate reduction for treatment of flue gas desulphurization wastewater from coal-fired power plant, J. Cleaner Prod., 228 (2019) 63–72.
[12] H.A. Elmawgoud, T.M. Elshiekh, S.A. Khalil, A.M. Alsabagh, M. Tawfik, Modeling of hydrogen sulfide removal from petroleum production facilities using H_2S scavenger, Egypt. J. Pet., 255 (2015) 131–137.
[13] G.A. Amin, S.A. Bazaid, M.A. El-Halim, A two-stage immobilized cell bioreactor with *Bacillus subtilis* and *Rhodococcus erythropolis* for the simultaneous production of biosurfactant and biodesulfurization of model oil, Pet. Sci. Technol., 31 (2013) 2250–2257.
[14] W.H. Zhu, Y. Li, Y. Gao, C. Wang, J. Zhang, H. Bai, T. Huang, A new method to fabricate the cathode by cyclic voltammetric electrodeposition for electro-Fenton application, Electrochim. Acta, 349 (2020) 400–415.
[15] J.G. Wynn, J.B. Sumrall, B.P. Onac, Sulfur isotopic composition and the source of dissolved sulfur species in thermo-mineral springs of the Cerna Valley, Chem. Geol., 271 (2010) 31–43.
[16] A.T. Jarullah, S.K. Aldulaimi, B.A. Al-Tabbakh, I.M. Mujtaba, A new synthetic composite nano-catalyst achieving an environmentally Friendly fuel by batch oxidative desulfurization, Chem. Eng. Res. Des., 160 (2020) 405–416.
[17] S. Tian, H. Mo, R. Zhang, P. Ning, T. Zhou, Enhanced removal of hydrogen sulfide from a gas stream by 3-aminopropyltriethoxysilane-surface-functionalized activated carbon, Adsorption, 15 (2009) 477–488.
[18] S.Y. Haruna, U.Z. Faruk, M.L. Gidado, Reduction of sulphur content of heavy crude oil using oxidative desulp, Am. J. Appl. Chem., 6 (2018) 15–20.
[19] M.A. Rezvani, M. Shaterian, M. Aghmasheh, Catalytic oxidative desulphurization of gasoline using amphiphilic polyoxometalate@polymer nanocomposite as an efficient, reusable, and green organic–inorganic hybrid catalyst, Environ. Technol., 41 (2020) 1219–1231.
[20] W.H. Zhu, R. Wang, T. Huang, F. Wu, The characteristics and two-step reaction model of p-nitroacetophenone biodegradation mediated by Shewanella decolorationis S^{12} and electron shuttle in the presence/absence of goethite, Environ. Technol., 35 (2014) 3116–3123.
[21] M. Kupczewska-Dobecka, S. Czerczak, J.P. Gromiec, K. Konieczko, Assessment of potential health hazards during emission of hydrogen sulphide from the mine exploiting copper ore deposit - case study, Cent. Eur. J. Public Health, 23 (2015) 137.
[22] N. Arancibia-Miranda, S.E. Baltazar, A. García, D. Muñoz-Lira, P. Sepúlveda, M.A. Rubio, D. Altbir, Nanoscale zero valent supported by zeolite and montmorillonite: template effect of the removal of lead ion from an aqueous solution, J. Hazard. Mater., 301 (2015) 371–380.
[23] W.H. Zhu, D. Yu, M. Shi, Y. Zhang, T. Huang, Quinone-mediated microbial goethite reduction and transformation of redox mediator, anthraquinone-2,6-disulfonate (AQDS), Geomicrobiol. J., 34 (2017) 27–36.